Electronic Supplementary Material (ESI) for Journal of Materials Chemistry A

Electronic Supplementary Information

Hollow polylactic acid microcapsules fabricated by gas/oil/water and bubble template methods

Daichi Sakurai,[a] Jay Jesus Molino Cornejo,[a] Hirofumi Daiguji,*[a] and Fumio Takemura[b]

[a] *Division of Environmental Studies, Graduate School of Frontier Sciences, The University of Tokyo, 5-1-5 Kashiwanoha, Kashiwa 277-8563, Japan*
[b] *Energy Technology Research Institute, National Institute of Advanced Industrial Science and Technology , 1-1-1 Higashi, Tsukuba 305-8565, Japan*

S1 Chemical potentials for each component in liquid and gas phases

If we assume that gas and liquid components form a weak solution in the liquid phase and an ideal mixture in the gaseous phase, then the explicit expressions for chemical potentials are as follows:

$$\mu_1'' = v_0 p_{01}'' + RT \ln\left(\frac{p_1''}{p_{01}''}\right), \qquad \text{(S1)}$$

$$\mu_2'' = \mu_{20}'' + RT \ln\left(\frac{p_2''}{p'}\right), \qquad \text{(S2)}$$

$$\mu_1' = v_0 p' + RT \ln\left(\frac{c_2'}{c_1' + c_2'}\right) = v_0 p' - RT \ln\left(1 + \frac{c_2'}{c_1'}\right) \approx v_0 p' - RT\left(\frac{c_2'}{c_1'}\right) \quad \text{at } c_2' << c_1', \qquad \text{(S3)}$$

$$\mu_2' = \mu_{20}' + RT \ln\left(\frac{c_2'}{c_{2s}'}\right), \qquad \text{(S4)}$$

where R and T are the gas constant and temperature, respectively; v_0, p''_{01}, and c'_{2s} are the specific volume of pure liquid, the saturation pressure of pure liquid, and the saturation concentration of the gas in the liquid phase, respectively; μ''_{20} and μ'_{20} are the chemical potentials of the gas in gaseous and liquid phases when the gas is dissolved up to the saturation concentration ($p''_2 = p'$ and $c'_2 = c'_{2s}$). From the equality of chemical potentials in liquid and gas phases for each component, i.e., $\mu''_1 = \mu'_1$ and $\mu''_2 = \mu'_2$, eqs 3 and 4 can be obtained.

S2 Stability of possible equilibrium states for bubbles in a closed volume of liquid

In our earlier study,[1] we obtained the condition for bubble stability from the differential of the total potential of a closed system of a liquid–gas solution containing q bubbles of radius r_b for the virtual displacement of equilibrium radius at constant p', T, and N_1. The condition for bubble stability was expressed as follows (eq 8 in Ref. 1):

$$q > \frac{3c_{01}' V' RT}{4\pi r_b^3 K_H}\left[\left(\frac{K_H}{p_1''} + \frac{p_1''}{K_H} - 2\right)\frac{3p_1'' p_2'' r_b}{2\gamma K_H} - \left(\frac{K_H}{p_2''} + \frac{p_1''}{K_H}\right)\frac{p_2''}{K_H}\right]^{-1}, \qquad \text{(S5)}$$

where K_H is the Henry's law constant. For a weak solution, the saturation concentration of air in the liquid phase, c'_{2s}, is given by

$$c_{2s}' = c_{01}' \frac{p'}{K_H}. \qquad \text{(S6)}$$

If the total molar amount of CH_2Cl_2, N_1, is explicitly shown using eq 1, the stability condition S5 is transformed as follows:

$$q > \frac{3N_1 RT}{4\pi r_b^3 K_H}\left[\left(\frac{K_H}{p_1''} + \frac{p_1''}{K_H} - 2\right)\frac{3p_1'' p_2'' r_b}{2\gamma K_H} - \left(\frac{K_H}{p_2''} + \frac{p_1''}{K_H} - \frac{p_1''}{p_2''}\right)\frac{p_2''}{K_H}\right]^{-1}. \qquad \text{(S7)}$$

Electronic Supplementary Material (ESI) for Journal of Materials Chemistry A

By using eqs 3–5, 7, 8, and S6, the stability condition S7 is transformed as follows:

$$\begin{aligned} &-\left(\frac{3N_1RT}{q4\pi r_\mathrm{b}^3 K_\mathrm{H}}+1-\frac{p_1''}{K_\mathrm{H}}\right)-\left(\frac{p_1''p_2''}{K_\mathrm{H}^2}-\frac{3r_\mathrm{b}p_2''}{2\gamma}\left(1-\frac{p_1''}{K_\mathrm{H}}\right)^2\right)>0 \\ &\left\{\frac{c_{2\mathrm{s}}'}{c_{01}'}\left(N_1-q\eta\frac{p_{01}''}{RT}\frac{4}{3}\pi r_\mathrm{b}^3\right)+q\frac{p'}{RT}\frac{4}{3}\pi r_\mathrm{b}^3\right\}\frac{d}{dr_\mathrm{b}}\left(1-\eta\frac{p_{01}''}{p'}+\frac{2\gamma}{r_\mathrm{b}p'}\right) \\ &+\frac{d}{dr_\mathrm{b}}\left\{\frac{c_{2\mathrm{s}}'}{c_{01}'}\left(N_1-q\eta\frac{p_{01}''}{RT}\frac{4}{3}\pi r_\mathrm{b}^3\right)+q\frac{p'}{RT}\frac{4}{3}\pi r_\mathrm{b}^3\right\}\left(1-\eta\frac{p_{01}''}{p'}+\frac{2\gamma}{r_\mathrm{b}p'}\right)>0 \\ &\frac{dN_2}{dr_\mathrm{b}}>0 \end{aligned} \tag{S8}$$

This result shows that the bubble is stable at $dN_2/dr_\mathrm{b} > 0$ for each N_2–r_b curve shown in Figs. 1a and 1b.

S3 Radius distributions of microbubbles in a droplet of CH_2Cl_2 solution of PLA

Figure S1 shows a bright-field image of microbubbles inside a droplet of CH_2Cl_2 solution of PLA (300 kDa) when the initial concentration of PLA in CH_2Cl_2 was 10 g L^{-1}. The central part of a droplet was observed just after sonication [see Fig. 3a (center)]. The bubble size was quite uniform and did not change considerably during the observation.

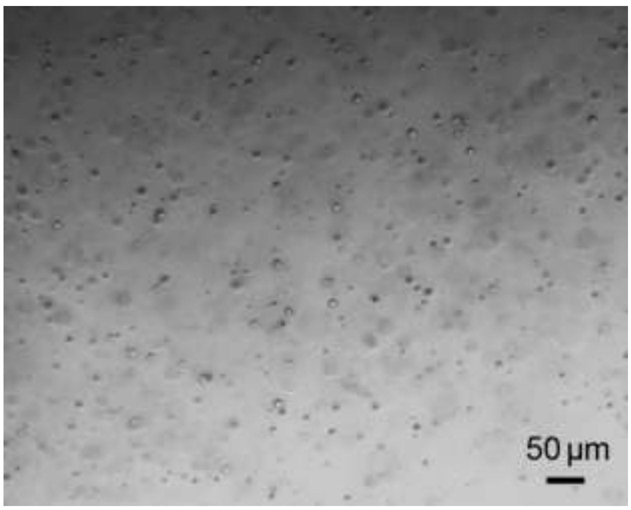

Fig. S1 Bright-field image of microbubbles inside a droplet of CH_2Cl_2 solution of PLA (300 kDa). The initial concentration of PLA in CH_2Cl_2 was 10 gL^{-1}.

Figure S2 shows the radius distributions of microbubbles in a droplet of CH_2Cl_2 solution of PLA (300 kDa). The initial concentrations of PLA in CH_2Cl_2 were 5, 10, and 20 g L^{-1}. The mean values (m), standard deviations (σ), and polydispersity indices (PI = standard deviation/mean) of the bubble radius for the initial concentrations of 5, 10, and 20 g L^{-1} were (m = 3.78 µm, σ = 1.23 µm, and PI = 32.5%), (m = 4.23 µm, σ = 1.26 µm, and PI = 29.8%), and (m = 6.34 µm, σ = 2.63 µm, PI = 41.5%), respectively. As the initial concentration of PLA increased, the size increased and the uniformity deteriorated.

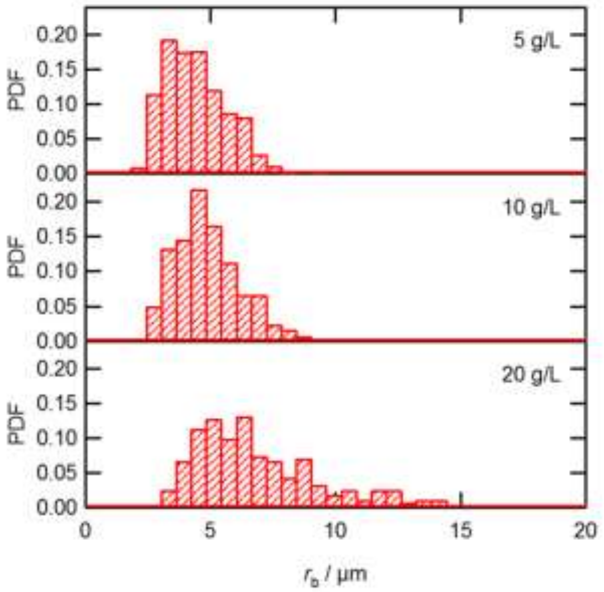

Fig. S2 Radius distributions of microbubbles in a droplet of CH_2Cl_2 solution of PLA (300 kDa). The initial concentrations of PLA in CH_2Cl_2 were 5, 10, and 20 g L^{-1}.

S4 Radius distribution of microdroplets of CH_2Cl_2 solution of PLA in an aqueous medium

Figure S3 shows a bright-field image of microdroplets of CH_2Cl_2 solution of PLA (300 kDa) in an aqueous medium after the droplet of CH_2Cl_2 solution of PLA and the surrounding aqueous solution of CH_2Cl_2 were mixed by a homogenizer for 10 s at 3500 rpm. The initial concentration of PLA in CH_2Cl_2 was 10 g L^{-1} and the initial concentration of CH_2Cl_2 in water was the saturation concentration at room temperature and atmospheric pressure. Each droplet contained several microbubbles.

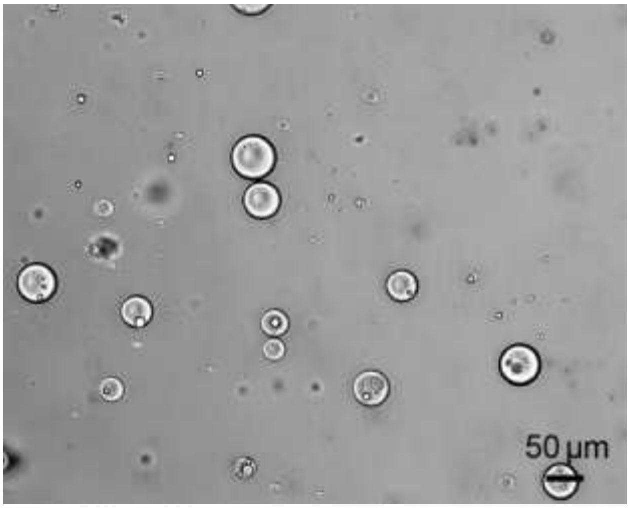

Fig. S3 Bright-field image of microdroplets of CH_2Cl_2 solution of PLA (300 kDa) in an aqueous medium after the droplet of CH_2Cl_2 solution of PLA and the surrounding aqueous solution of CH_2Cl_2 were mixed by a homogenizer for 10 s at 350 rpm. The initial concentration of PLA in CH_2Cl_2 was 10 g L^{-1} and the initial concentration of CH_2Cl_2 in water was the saturation concentration at 1 atm and room temperature.

Figure S4 shows the radius distributions of microdroplets of CH_2Cl_2 solution of PLA (300 kDa) in an aqueous medium when the droplet of CH_2Cl_2 solution of PLA and the surrounding aqueous solution were mixed by a homogenizer for 10 s at 2500, 3500, and 4500 rpm. The mean values (m), standard deviations (σ), and polydispersity indices (PI = standard deviation/mean) of the microdroplet radii for rotation speeds of 2500, 3500, and 4500 rpm were (m = 16.9 µm, σ = 7.12 µm, and PI = 41.2%), (m = 13.6 µm, σ = 8.73 µm, and PI = 64.4%), and (m = 14.3 µm, σ = 8.46 µm, PI = 59.2%), respectively. As the rotation speed increased from 2500 to 3500 rpm, the size increased and the uniformity deteriorated, but the data for 3500 and 4500 rpm were close to each other.

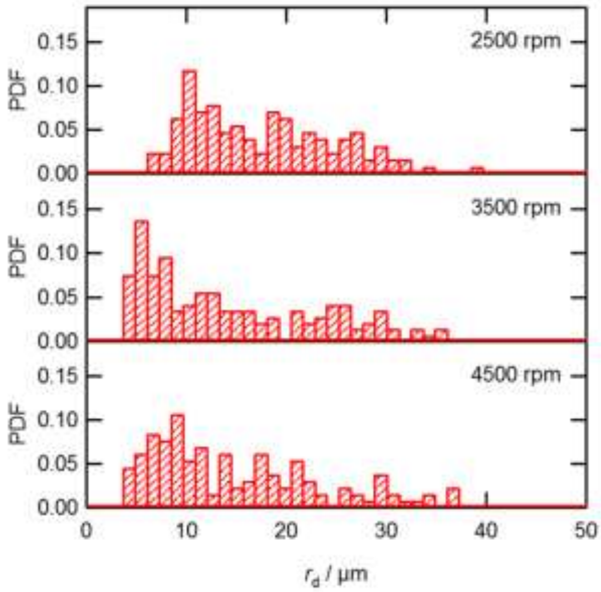

Fig. S4 Radius distributions of microdroplets of CH_2Cl_2 solution of PLA (300 kDa) in an aqueous medium when a droplet of CH_2Cl_2 solution of PLA and the surrounding aqueous solution were mixed by a homogenizer for 10 s at 2500, 3500 and 4500 rpm. The initial concentration of PLA in CH_2Cl_2 was 10 g L^{-1}.

REFERENCES

(1) H. Daiguji, S. Takada, J. J. Molino Cornejo and F. Takemura, *J. Phys. Chem. B* 2009, **113**, 15002–15009.